Journal of Earth Sciences and Geotechnical Engineering, vol.7, no. 1, 2017, 151-173
ISSN: 1792-9040 (print version), 1792-9660 (online)
Scienpress Ltd, 2017

A sensitivity study of road transportation emissions at metropolitan scale

Ruiwei Chen[1], Vincent Aguiléra[2], Vivien Mallet[3], Florian Cohn[4], David Poulet[5] and Fabien Brocheton[6]

Abstract

Road traffic transportation emissions depend on both the traffic flow and the vehicles emission factors. They are very sensitive to the input data of both traffic assignment models and emissions calculation methods. In this study, we investigate the influences of the input data on a simulation chain from traffic flow assignment to emissions calculations, based on a case study in the agglomeration of Clermont-Ferrand in France. In order to better represent the congestion phenomenon and the temporal and spatial evolution of traffic flow, we use a dynamic traffic assignment model, LADTA, to compute the traffic flow at street resolution. The model is evaluated by comparison between model predictions and traffic flow observations captured by inductive loop traffic detectors. The traffic flow outputs of LADTA are then coupled with COPERT model to calculate emissions of air pollutants (nitrogen oxides NOx for example). A sensitivity study is then carried out by varying the input parameters in the traffic emission modeling chain: the total traffic volume injected into the network, the average speed, the vehicle fleet composition, etc. The study shows that the emissions are very sensitive to these factors, especially during the transition from a free traffic network to a congested one.

Keywords: road traffic emissions, dynamic traffic assignment, COPERT, sensitivity study, congestion

[1] CEREA, joint laboratory École des Ponts Paris Tech/EDF R&D, Université paris-Est. E-mail: ruiwei.chen@enpc.fr
[2] CEREMA. E-mail : vincent.aguilera@cerema.fr
[3] INRIA. Email : vivien.mallet@inria.fr
[4] NUMTECH. E-mail : florian.cohn@numtech.fr
[5] NUMTECH. E-mail : poulet@numtech.fr
[6] NUMTECH. E-mail : fabien.brocheton@numtech.fr

1 Introduction

The emissions of road traffic are one of the main sources of air pollutants in urban area. In Île-de-France for instance, the road traffic is responsible for more than 55% of nitrogen oxides (NOx) and more than 30% of particulate matter [1]. To analyze how traffic influences the air pollutant emissions at an agglomeration scale, traffic assignment models are needed for predicting the traffic volume at street resolution. There exist both static and dynamic traffic assignment models to reach this goal. The resulting traffic information is then used in emission calculation methods to estimate the air pollutants emitted by road traffic.

Our study focuses on the sensitivity of the emissions calculation outputs to the inputs of a dynamic traffic assignment model. The latter lets we better understand the effects of congestions resulting from the temporal evolution and time-dependent interactions of traffic flows. This paper is divided into 4 sections. The first section (Section 2) recalls the fundamentals of traffic assignment models, and presents briefly the dynamic traffic assignment (DTA) model, LADTA (for Lumped Analytical DTA), that we use in this study. Section 3 presents an analysis of the real-time traffic measurement data in Clermont-Ferrand, in order to study the road network users' behaviors and prepare the input data for LADTA simulation. Section 4 presents the main results from the simulation of traffic assignment and emission calculation, in the agglomeration of Clermont-Ferrand. Finally, the sensitivity analyses are presented in Section 5.

2 Description of Traffic Assignment Model and Emissions Model

Traffic assignment aims at determining the network traffic flows according to network users' route choices when they travel from their origins to their destinations. It can also be considered as an economical equilibrium between the demand and the supply. The Origin-Destination matrix (O-D matrix) describes the total flux from original zones to destination zones. The road network shows limited capacities to absorb all the demand. One of the main hypotheses for traffic assignment problems is that every network user makes their route choice by minimizing their own travel cost, such as travel time, toll, etc. The cost is often converted to one general criterion, such as time, which is called generalized cost of route choice. At equilibrium when every traveler succeeds in finding an optimal route, all used routes associated with the same O–D pair should have the same minimum generalized cost, so that there is no possibility for users to shift to another route. This is the user equilibrium condition [2], and it was proved to be adequate for both static and dynamic traffic assignment models, with a certain number of assumptions [3] [4] [5].

In both static and dynamic traffic assignment models, the travelers are assumed to

have complete information about each link in a network (the supply): physical capacity, length, speed limit and toll price (if any), in order to estimate the generalized travel cost of each available route. In a static model, the effect of road capacity on travel time is modeled by a volume-delay function (VDF): the travel cost (or time) is a strictly increasing function of the traffic volume. For example, the Bureau of Public Roads [6] in the USA proposed a commonly used function as Equation (1),

$$t = t_0[1 + \alpha(V/C)^{\beta}] \quad (1)$$

where t is the link travel time to determine, t_0 is the link free flow travel time, V is the volume on the link, C is the capacity, α and β are coefficients to be adjusted. Figure 1 illustrates this type of VDFs with $\alpha = 1$ and a varying β. It is observed that VDFs are very sensitive to β. To represent the fact that the link travel time increases with the volume loaded on a link in congested cases, the volume may increase indefinitely and exceed the link capacity. This is not possible in reality, and it is also unrealistic to assume that the travel cost depends only on the flow of the link. In other words, in congested condition, the travel time calculated by VDF in static models does not depend on physical features of congestion (such as travel speed, density, or queue) [7]. This is a motivation to seek for dynamic traffic assignment models (DTA) in order to better represent the congestion phenomenon.

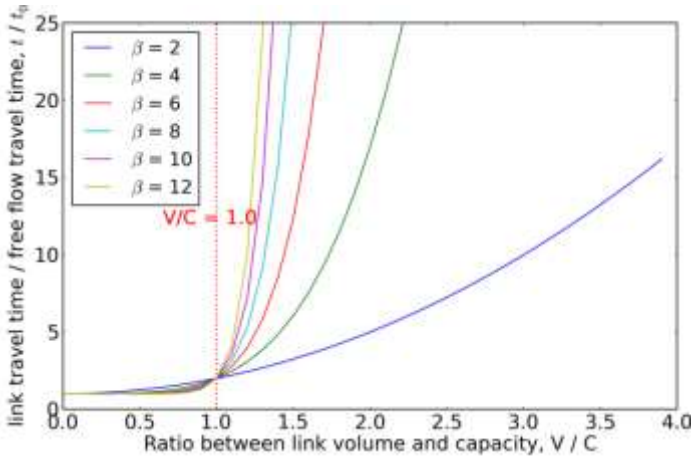

Figure 1: An example of volume delay functions in static traffic assignment models. When volume loaded on a link exceeds the capacity, the link travel time (t) can be calculated with $\alpha = 1$ and different β.

In dynamic assignment, the speed decreases when the link density increases, and the link travel time will therefore increase. The link travel time also depends on the vehicles' entrance time on the network. In fact, the traffic already existing on the link can decrease the link capacity. This may result in an increase of link travel

time if the actual inflow volume exceeds the actual capacity of the link. There are different methods to calculate the link travel time in DTA, such as the fundamental diagram of traffic flow to represent the density – speed relationship [8] [9] [10]. Another method is bottleneck modeling where queue appears in upstream junction when the volume assigned to the link exceeds the capacity [11]. In this model, the time spent in queue is taken into consideration to compute the link travel time.

Since the traffic emissions depend on both the traffic volume and the average speed of the vehicles and these two factors are correlated when congestion appears, a DTA model is used in our study to better represent and analyze the sensitivity of traffic emissions.

2.1 Introduction of LADTA

The LADTA model is one of the link-time-based DTA models which can be applied to a large-scale real network. Together with its software, LADTA ToolKit (LTK), it can handle the DTA problem of a metropolitan network frame within a reasonable time [4]. It needs a dynamic O-D matrix as input data, as well as full information of the network. Then it computes the dynamical user equilibrium between the supply and the demand. Its outputs are the traffic flow and travel time for every link. The calculation of link travel time is based on bottleneck model.

2.2 COPERT IV method for calculations of emission factors

To calculate the traffic emissions, the tier 3 method of EMEP/EEA (2013) [12] is used. The total exhaust emissions from road transport are calculated as the sum of hot emissions and cold-start emissions. In this study, only exhaust hot emissions from passenger cars are considered.

For each link in the network, the hot emissions can be estimated by the following equation:

$$\mathrm{E_{hot,i,j}(g)} = \mathrm{e_{hot,i,j}(g \cdot km^{-1})} \times \mathrm{N_j(veh)} \times \mathrm{M_j(km \cdot veh^{-1})} \quad (2)$$

where $\mathrm{E_{hot}}$ is the link's hot emission of a certain type of pollutanti, and a certain vehicle type j, $\mathrm{e_{hot}}$ is the hot emission factor for the corresponding pollutanti and vehicle type j, N is the vehicle number of vehicle type j on this link, and M is the distance traveled by this corresponding category of vehicles.

The vehicle number of each link can be obtained by traffic assignment models, and the distance traveled by vehicles is link length. The hot emission factors for each pollutant and each category of vehicles are calculated according to the COPERT IV method in EMEP/EEA 2013 [12]. Briefly speaking, the hot emission factors mainly depend on vehicle's average speed and the vehicle fleet.

2.3 The simulation scenario from traffic flow assignment to emission calculations

With the help of a static O-D matrix during evening peak period, a dynamic O-D matrix is built by applying a daily temporal evolution profile of the traffic flow in Clermont-Ferrand, as observed by the inductive loop traffic detectors in the network. A LADTA simulation can be launched for a complete day, and the traffic flow of each interval of simulation (15 minutes) can be obtained as well as the link travel time. The link travel time resulting from LADTA model is used in calculating the average travel speed on each link. Using the vehicle fleet composition data and the flow data of LADTA model, the air pollutant emissions can be calculated for each 15 minutes during a full day.

3 Analyses on Real-time Traffic Flow Observational Data of Clermont-Ferrand

3.1 Description of stationary inductive detectors in road network of Clermont-Ferrand

Clermont-Ferrand has 535 inductive loop traffic detectors in the road network, which are generally located in main city boulevards and/or crossroads, as presented in Figure 2. They collect the traffic density and flow information every minute. These precious and rich traffic data help us analyze the network users' behavior and set up the LADTA simulation. The City of Clermont-Ferrand has provided two years of observational data of every detector with a resolution of 15 minutes, from September 2013 to September 2015 (included). The data for the first year have been analyzed in detail in order to set up and calibrate LADTA model, and the data for the second year are then used to evaluate the traffic flow results predicted by LADTA.

Figure 2: Detector locations in Clermont-Ferrand. The blue lines represent the roads of Clermont-Ferrand. The yellow arrows represent the position and direction of traffic detectors.

3.2 The analysis of observational data

The observational data of the real road traffic help us better understand the

behaviors of road network users. It is observed that the network users in Clermont-Ferrand almost always behave the same for the same day type. Figure 3 shows temporal evolution profiles of flow for each Tuesday during 2013.9 – 2014.9.

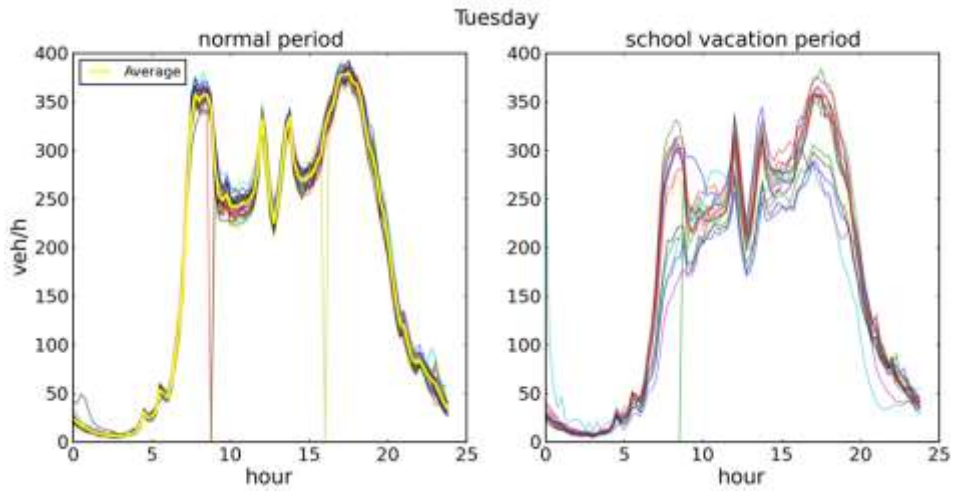

Figure 3: Temporal profiles of traffic flow averaged over all detectors of all Tuesdays. Each thin line represents a temporal profile of traffic on each Tuesday during normal periods (left) and scholar vacation periods (right), during 2013.9 – 2014.9, and the yellow line on the left profile is the average temporal profile of traffic flow over all Tuesdays in normal periods. Several points reach zero when no data was collected. This rarely happens (less than 5%), and the data in these cases have not been taken into account for calculating of average temporal profile.

The left profile in Figure 3 presents the temporal profile of traffic during a normal period. The right profile is the traffic during vacation period. It is clear that for every working day, the morning peak appears almost at the same moment of the day around 08:00, so is the evening peak, around 17:00. The differences among traffic flows during peak hours of different days are not significant. Moreover, the total volume of traffic during a day remains almost unchanged from one Tuesday to another. The same feature is observed for other weekdays, and the temporal profile of the same weekday during a year can be easily represented by an average temporal profile (yellow line). Furthermore, it is also shown in the Figure 4 that the total daily volume of the traffic slightly changes from Monday to Friday, but remains quite stable from month to month during non-vacation periods. This allows us to simplify the construction of dynamic O-D matrix for LADTA. However, as shown in the right profile in Figure 3 and daily volume in Figure 4, during the vacation period, the total daily volume and the temporal profile of the traffic are harder to predict, and the traffic flow during peak hours are not the same. It would not be reasonable to represent these days by only one temporal

profile, and individual profiles should be used when simulating the traffic flow of these days.

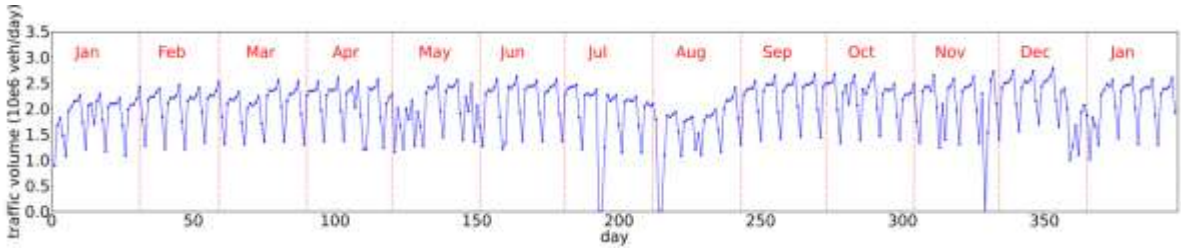

Figure 4: Daily traffic volume measured during the year 2014 (in 10^6 veh/day). The value of each point shows the sum of observational data of all detectors during each day. The value reaches zero when no data was collected.

In the following sections, the case study is for a working Tuesday during non-vacation period for the agglomeration of Clermont-Ferrand.

4 Traffic Assignment and Emission Calculations for Agglomeration of Clermont-Ferrand

4.1 Input data

The traffic demand and the physical road network supply in the traffic assignment problem need to be mathematically modeled respectively by an oriented graph with nodes and links, and an O-D matrix of traffic demand flux between each O-D pair. Figure 5 presents the modeled domain of the agglomeration of Clermont-Ferrand for LADTA. The simulation results will be presented only on red rectangle domain.

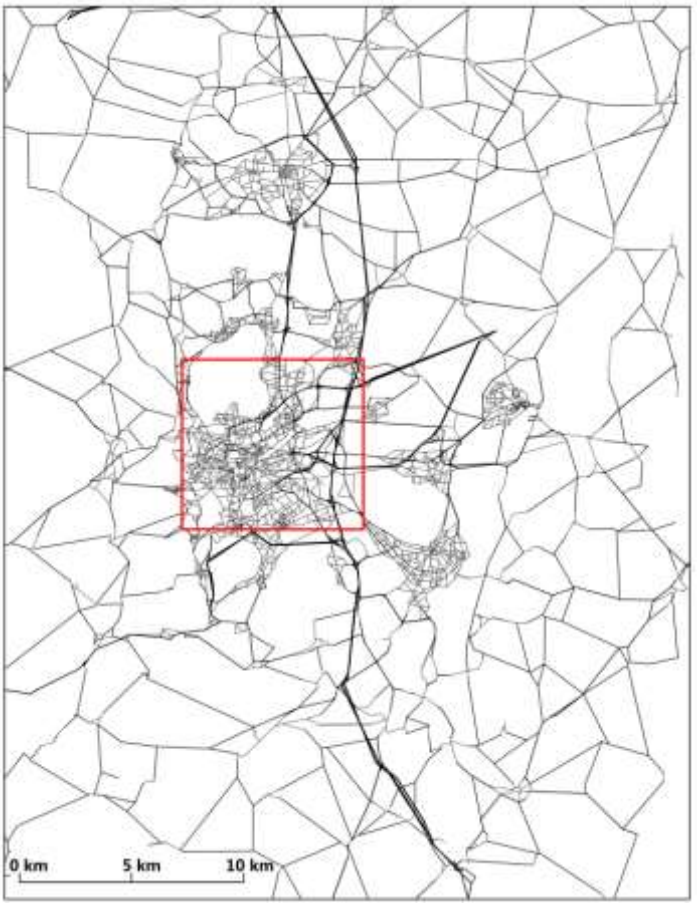

Figure 5: Modeled network for LADTA simulation. The road network of Clermont-Ferrand is modeled by links and nodes. Bold lines represent links with a capacity higher than 1600 veh/h, e.g. highways, national roads, departmental roads, etc.

(1) Zoning and dynamic OD matrix

The whole simulation domain is divided in 124 zones, and the O-D matrix of traffic demand during the evening rush hour is already given by the Syndicat Mixte des Transport en Commun de l'agglomération Clermontoise (SMTC – Clermont-Ferrand). Then, we use the temporal evolution of a typical day, a Tuesday during working week (as in Figure 3, left) to generate our dynamic O-D matrix for LADTA simulation. This temporal profile is calculated by the observational data during the period from September 2013 to June 2014. The starting hour of simulation is from 03:15 to minimize errors, since this is the time when the total traffic volume in the network is minimum, and LADTA model has to assign the network from zero vehicle.

(2) Oriented graph to model the road network

For the agglomeration of Clermont-Ferrand, the modeled network in the simulation domain has 19628 links and 8844 nodes. There is detailed information

for each link, including its head node, tail node, length, capacity, speed limit and number of lanes. The free flow travel time is calculated from the link's length and speed limit.
With these two main input data, a LADTA assignment simulation is then launched for a complete day. The results and the corresponding statistical analysis are presented in the next sub-section.

4.2 Traffic assignment results simulated by LADTA model

4.2.1 Temporal evolution and vehicle travel time during 24h

Figure 6 shows the average temporal evolution of the traffic during 24h. The flow results are averaged over of all inductive loop detectors. The LADTA simulation results have been compared with observational data during the period from September 2014 to June 2015. This shows that LADTA can very well simulate the temporal profile.

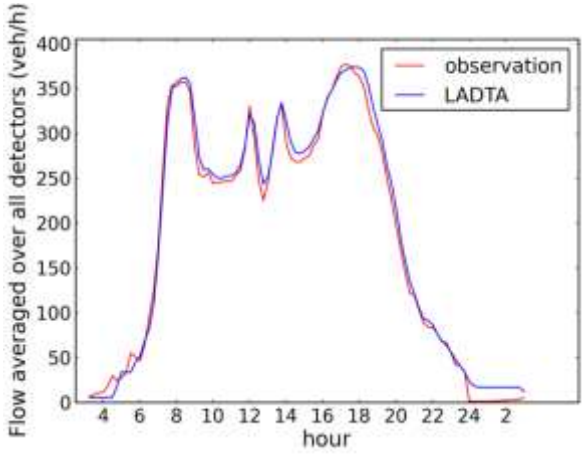

Figure 6: Temporal profile of spatial average flow on a normal Tuesday during non-vacation periods from 2014/09/01 to 2015/06/30.

4.2.2 Spatial distribution of the traffic in the network

Figure 7 and Figure 8 show the traffic assignment and the congestion distribution of Clermont-Ferrand from 07:00 to 08:30, for each 15 minutes. In this section, a link is considered to be congested when the associated average travel time (t) is 50% more than its free flow travel time (t0).The results show the links with higher capacities have been assigned more traffic volume, and the congestions appear firstly and more frequently on crossroads. These fit well to the reality of urban traffic situation. The spatial distributions at different time periods show that the transition to the morning peak is almost immediate, and some links become congested within a quarter of an hour. Moreover, from 07:45 to 08:30, no significant difference can be seen in Figure 7 for traffic flows, as they have

already reached the maximum, i.e. the link capacity. However, Figure 8 shows that during the same period, the link travel time continues increasing and there are more and more congested links. This congestion phenomenon may affect the emissions, since the latter depend on both the vehicle number and the average travel time. The dynamic traffic assignment model can then give more detailed information of traffic temporal evolutions than the static assignment model.

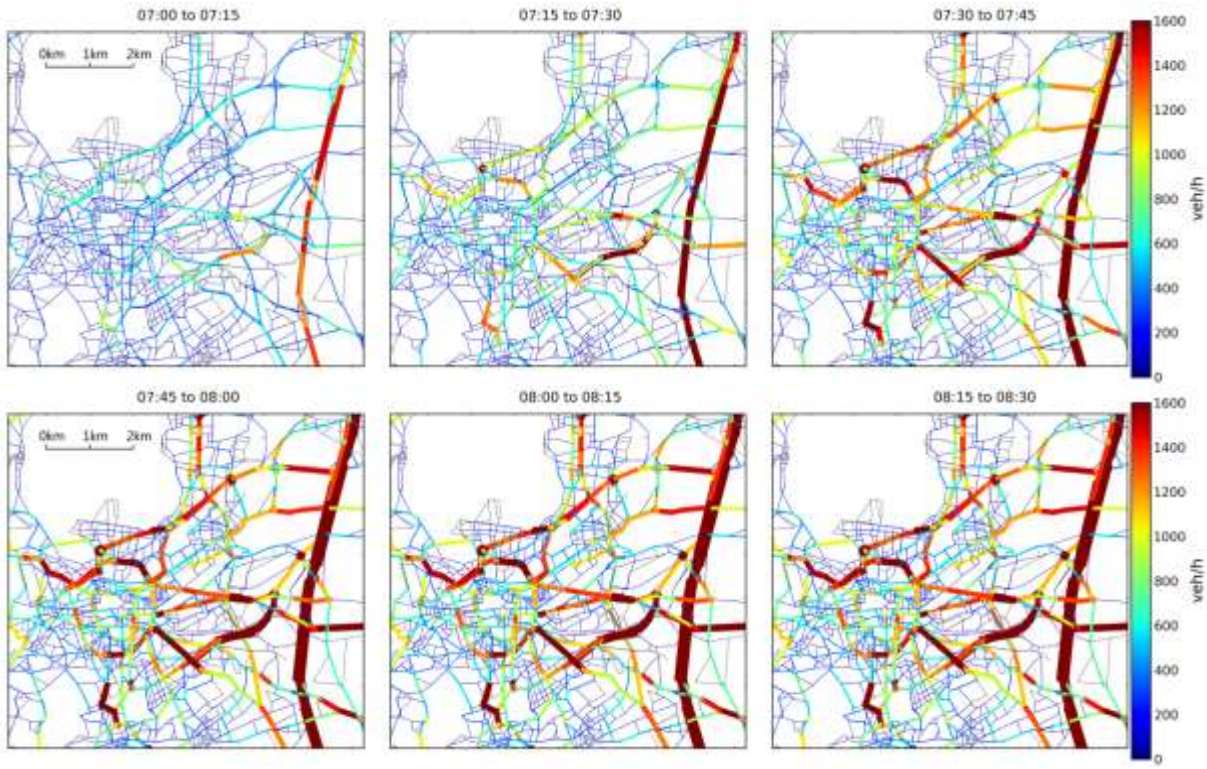

Figure 7: The traffic assignment results of LADTA from 07:00 to 08:30. Black lines represent unused links. The line width is proportional to the traffic flow on the link.

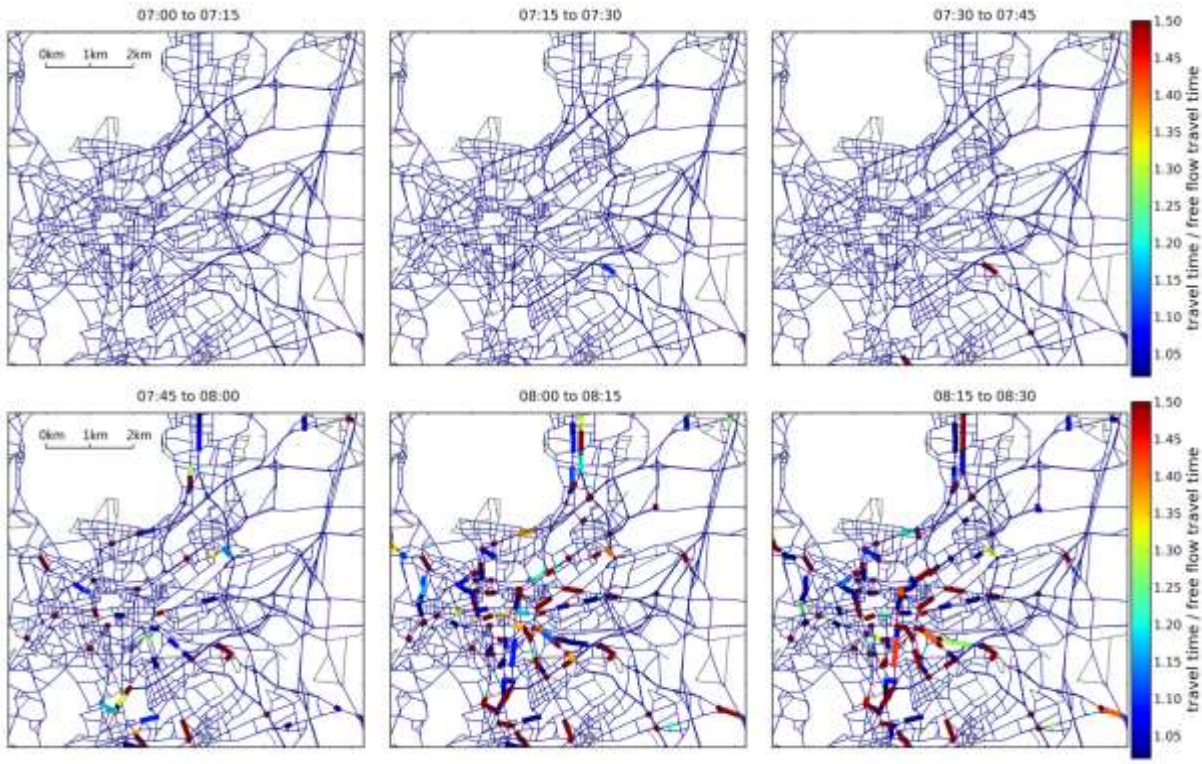

Figure 8: The spatial distribution of congestion from 07:00 to 08:30. Black lines represent unused links. Thin blue lines represent links whose travel time equals to its free flow travel time. Bold lines with various colors represent links with travel time larger than its free flow travel time.

4.2.3 Comparison of simulation results and observational data

With the coordinate information, we can determine the corresponding link in the modeled network for each detector. One detector can only collect data of one lane and there may be several detectors on the same link. If we divide the simulated traffic flow of each link by its lane number, we can obtain the simulated traffic flow for each detector, for each 15 minutes during the day. For observational data, we have M detectors, N Tuesdays and T time steps during the day. The total size of observational data is $M \times N \times T$. We assume that for each detector, the simulation results are the same at the same time for each Tuesday. Then we can build the simulation data sequence of the same size as observational data, i.e. $M \times N \times T$. Table 1 shows the statistical values and scores for evaluating the model, where $o_{m,n,t}$ is the observed sequence and $s_{m,n,t}$ is the corresponding simulated sequence.

Table 1: Statistical values and scores for evaluation of LADTA.

Statistical values	Formula
Global mean value	$\overline{o}_{global} = \frac{1}{M \times N \times T}\left(\sum_{m=1}^{M}\sum_{n=1}^{N}\sum_{t=1}^{T} o_{m,n,t}\right)$
	$\overline{s}_{global} = \frac{1}{M \times N \times T}\left(\sum_{m=1}^{M}\sum_{n=1}^{N}\sum_{t=1}^{T} s_{m,n,t}\right)$
Spatial average flow sequence	$\overline{o}_{spatial}^{(t)} = \frac{1}{M \times N}\left(\sum_{m=1}^{M}\sum_{n=1}^{N} o_{m,n,t}\right),\ \overline{s}_{spatial}^{(t)} = \frac{1}{M \times N}\left(\sum_{m=1}^{M}\sum_{n=1}^{N} s_{m,n,t}\right)$
Temporal average flow sequence	$\overline{o}_{temporal}^{(m)} = \frac{1}{N \times T}\left(\sum_{n=1}^{N}\sum_{t=1}^{T} o_{m,n,t}\right)$
	$\overline{s}_{temporal}^{(m)} = \frac{1}{N \times T}\left(\sum_{n=1}^{N}\sum_{t=1}^{T} s_{m,n,t}\right)$
Mean bias error	$e_{global} = \frac{1}{M \times N \times T}\sum_{m=1}^{M}\sum_{n=1}^{N}\sum_{t=1}^{T}(s_{m,n,t} - o_{m,n,t})$
	$e_{temporal} = \frac{1}{T}\sum_{t=1}^{T}\left(\overline{s}_{spatial}^{(t)} - \overline{o}_{spatial}^{(t)}\right)$
	$e_{spatial} = \frac{1}{M}\sum_{m=1}^{M}\left(\overline{s}_{temporal}^{(m)} - \overline{o}_{temporal}^{(m)}\right)$
Root mean square error (RMSE)	$RMSE_{global} = \sqrt{\frac{1}{M \times N \times T}\sum_{m=1}^{M}\sum_{n=1}^{N}\sum_{t=1}^{T}(s_{m,n,t} - o_{m,n,t})^2}$
	$RMSE_{temporal} = \sqrt{\frac{1}{T}\sum_{t=1}^{T}\left(\overline{s}_{spatial}^{(t)} - \overline{o}_{spatial}^{(t)}\right)^2}$
	$RMSE_{spatial} = \sqrt{\frac{1}{M}\sum_{m=1}^{M}\left(\overline{s}_{temporal}^{(m)} - \overline{o}_{temporal}^{(m)}\right)^2}$

Normalized mean square error (NRMSE)	$\frac{\mathrm{RMSE}}{\overline{o}}$
Correlation	$R_{global} = \frac{\sum_{m=1}^{M}\sum_{n=1}^{N}\sum_{t=1}^{T}\left[\left(s_{m,n,t}-\overline{s}_{global}\right)\left(o_{m,n,t}-\overline{o}_{global}\right)\right]}{\sqrt{\sum_{m=1}^{M}\sum_{n=1}^{N}\sum_{t=1}^{T}\left(s_{m,n,t}-\overline{s}_{global}\right)^2}\sqrt{\sum_{m=1}^{M}\sum_{n=1}^{N}\sum_{t=1}^{T}\left(o_{m,n,t}-\overline{o}_{glo}\right.}$ $R_{temporal} = \frac{\sum_{t=1}^{T}\left[\left(\overline{s}_{spatial}^{(t)}-\overline{s}_{spatial}\right)\left(\overline{o}_{spatial}^{(t)}-\overline{o}_{spatial}\right)\right]}{\sqrt{\sum_{t=1}^{T}\left(\overline{s}_{spatial}^{(t)}-\overline{s}_{spatial}\right)^2}\sqrt{\sum_{t=1}^{T}\left(\overline{o}_{spatial}^{(t)}-\overline{o}_{spatial}\right)^2}}$ $R_{spatial} = \frac{\sum_{m=1}^{M}\left[\left(\overline{s}_{temporal}^{(m)}-\overline{s}_{temporal}\right)\left(\overline{o}_{temporal}^{(m)}-\overline{o}_{temporal}\right)\right]}{\sqrt{\sum_{m=1}^{M}\left(\overline{s}_{temporal}^{(m)}-\overline{s}_{temporal}\right)^2}\sqrt{\sum_{m=1}^{M}\left(\overline{o}_{temporal}^{(m)}-\overline{o}_{tempor}\right.}$

LADTA is evaluated with the observational data sequence of all Tuesdays during non-vacation period from September 2014 to June 2015. The statistical scores of LADTA model are presented in Table 2. It is shown that LADTA model can well predict the temporal evolution of the daily traffic. The model performed perfectly with high correlation and low bias or RMSE. However, the model has limitations to predict the spatial distribution of the traffic in the network. This may be due to at least three reasons: (i) the method to estimate the simulated results for each detector by dividing link volume with lane number, ignoring that left side lanes and right side lanes might have different traffic flows, (ii) the hypotheses that all the travelers choose their route by minimizing their generalized travel cost, while different users may use several different criteria for routing in reality, (iii) the nature of origin – destination pairs according to the nature of zones. Indeed, the temporal evolution profile of LADTA inputs might be different for an O-D pair from an industrial zone to a residence zone, and for a pair from a residence zone to an industrial zone.

Table 2: Comparison of traffic flow results between LADTA and measurements.

	Global	Temporal	Spatial
RMSE (veh / h)	149	12	112
Mean bias error (veh / h)	6	6	5
Mean value of observations (veh / h)	183	183	183
NRMSE (%)	81.4	6.6	61.2
Correlation	0.73	0.99	0.57

The results of LADTA are then used in calculations of the emissions for air pollutant at street resolution in agglomeration of Clermont-Ferrand, combining with links' information and vehicle fleet data.

4.3 Calculation of air pollutant emissions for agglomeration of Clermont-Ferrand

The national vehicle fleet composition data of 2013 have been used in the calculation of emissions, as shown in Table 3 and Table 4. Using the average travel time on each link, the traffic flow results from LADTA, and the link length, the hot emissions of nitrogen oxides (NOx) emitted by passenger cars are calculated, during each 15 minutes for a normal working day. The results are presented in Figure 9.

Table 3: Distribution of engine type and capacity [13].

Engine type		Engine capacity	Percentage within each category (in %)
Gasoline	29.2%	< 1.4 L	59.9
		1.4 – 2 L	34.6
		> 2L	3.8
Diesel	70.6%	< 1.4 L	9.8
		1.4 – 2 L	77.8
		> 2L	12.5

Table 4: Composition of the vehicle fleet for passenger cars according European emission standards, i.e. the Euro standard [13].

Euro standard	Percentage (in %)
Pre Euro	3.6
Euro 1	6.6
Euro 2	14.0
Euro 3	33.5
Euro 4	39.9
Euro 5	2.4

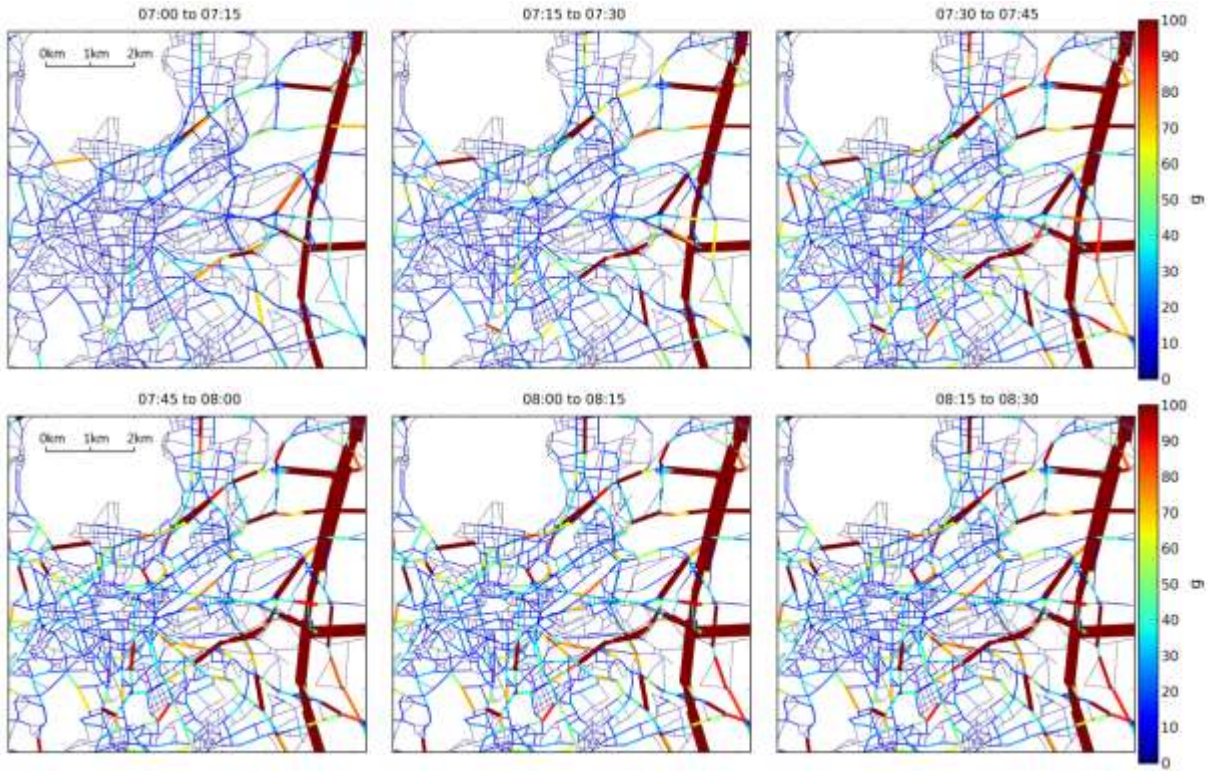

Figure 9: Emission map of NOx in Clermont-Ferrand during 07:00 – 08:30. Black lines represent links with zero emission. The line width is proportional to the traffic flow on the link.

In Figure 9, we can see that the highways are the most polluted links in the network since there is more traffic and the speed is higher. During the transition from normal period to rush hours, the emissions of NOx change with the evolution of time, and the spatial distribution of emissions has also changed. It is also observed that the emissions are very sensitive to the traffic flow affected in the network, and the sensitivity studies are presented in the next section.

5 Sensitivity Analyses

In this section, we are interested in three main factors for calculating emissions: the total traffic demand in the network, the vehicle average speed and the vehicle fleet composition. The results in Section 4 are considered as references. We take three outputs as indicators: the total vehicle travel time, the proportion of congested links and the total NOx emissions in the whole network. For the second indicator, a link is considered as congested with the same criterion as in Section 4: travel time 50% higher than the free flow travel time. The congestion proportion is then calculated as the ratio between the total length of congested roads in the network, and the total length of the whole network.

5.1 The total demand of traffic volume in the network

We vary the total demand volume from – 50% to + 100 %, with the same temporal profile as for dynamic O-D matrix as Section 4. The data for links' information and vehicle fleet composition remain unchanged. Then the vehicle travel time, the proportion of congested roads in the whole network, and the emissions are calculated for each link during each 15 minutes.

The Figure 10 shows the spatial distribution of these three indicators during the period from 07:45 to 08:00, with a total traffic demand volume of – 50%, 0% and + 50% comparing with the referenced simulation case in Section 4. It can be observed that the traffic volume and the link travel time are more influenced by the evolution of the total demand volume entered to the LADTA model than the link emissions. In order to analyze the sensitivity in detail, the total values of these indicators of the whole network during 24 h are calculated for each case with different total demand volume. The sensitivity analyses of these three global indicators are presented from Figure 11 to Figure 13.

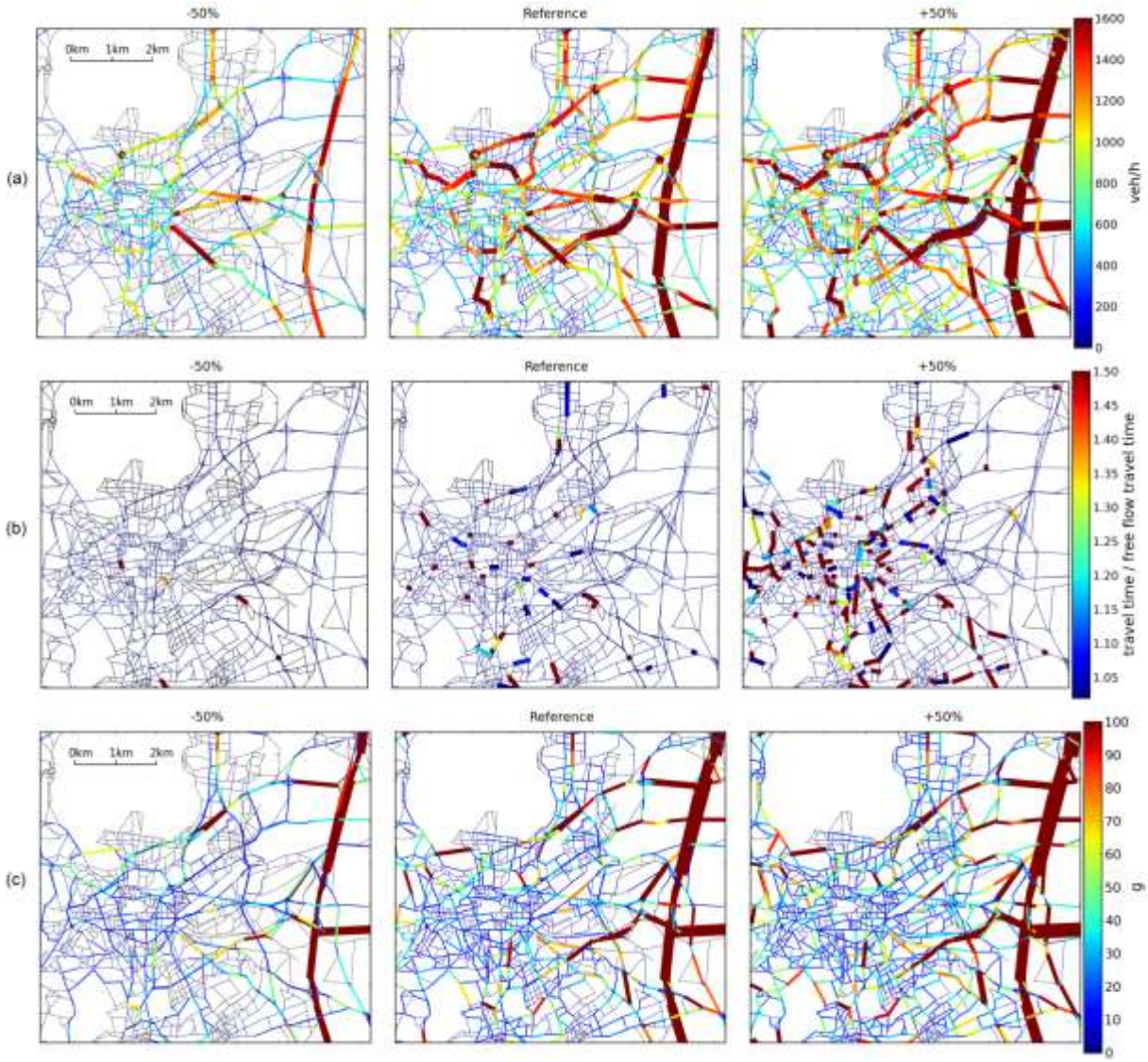

Figure 10: The spatial distribution of (a) traffic flow, (b) congestion and (c) emission of NOx during 07:45 to 08:00, with change of total demand volume of – 50%, reference case, and + 50 %. Black lines represent unused links in LADTA model. The line width is proportional to link's vehicle travel time in (a) and to link's emission in (c). In (b), thin blue lines represent links where the travel time equals to the free flow travel time.

Figure 11 to Figure 13 show the influence of the total traffic demand volume on the three outputs. We see that the total vehicle travel time and the congestion rate of the network are very sensitive to the total demand volume, especially when congestion phenomenon appears. Figure 11 and Figure 12 show that the total vehicle travel time and the network's congestion proportion become about 10 times higher than the reference case, when the total demand is doubled. In Figure 11 (b) and Figure 12 (b), below the reference total demand volume, the increase of vehicle travel time and the congestion rate is almost linear with the increase of the

demand. After that, the network becomes more and more congested and the growth of travel time of vehicles becomes increasingly fast.

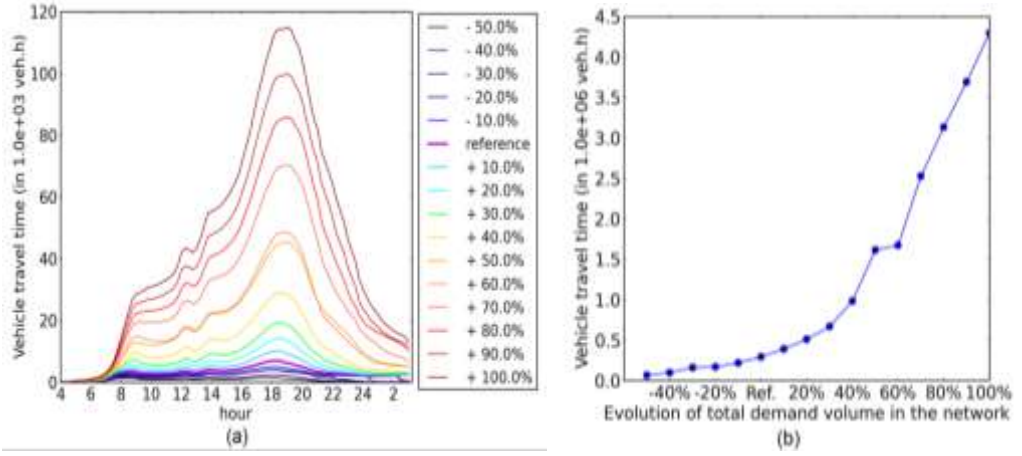

Figure 11: Sensitivity of vehicle travel time to the total demand volume. (a) Evolution during the day (in 10^3 veh·h), (b) evolution of the total vehicle travel time in the whole network (in 10^6 veh·h).

Furthermore, it is interesting to notice that the road traffic during the evening peak period is more congested than during the morning peak, and travelers suffer a longer travel time during evening peak with congestions. The network before evening peak hour is no longer empty and the traffic appearing before evening peak can affect the dynamic assignment traffic results. This is the phenomenon that we can only observe in DTA models. In fact, the existing traffic before evening peak hours might decrease the link capacity, and the capacity varies with the increase of traffic demand when peak hour arriving. This phenomenon cannot be simulated by static traffic assignment models even with separate time periods since the static models do not take into account the existing traffic on the network, and there is no interaction between traffic flow assigned and the link capacity.

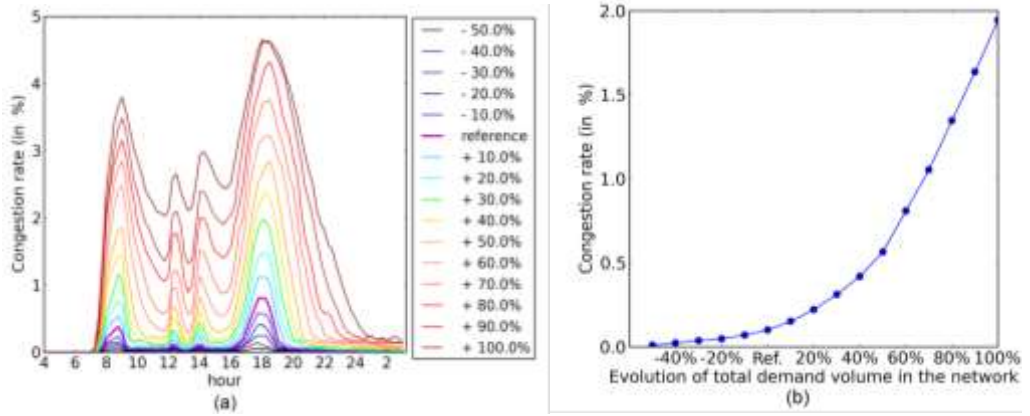

Figure 12: Sensitivity of the congestion rate to the total demand volume (in %). (a) evolution during the day, (b) evolution of the proportion of congested links in the whole network.

Concerning the total emission, as shown in the Figure 13, the influence of the total volume is not linear either, but the non-linearity of the total emissions is not as obvious as in the vehicle travel time. The total emissions tripled when we double the total demand volume comparing with the reference case. In fact, the emission factor of NOx changes with the average travel speed as shown in Figure 14. With the increase of traffic volume, roads are becoming congested and the travel time increases. This leads to the decrease of vehicle speed, and decrease of emission factors for most of the links.

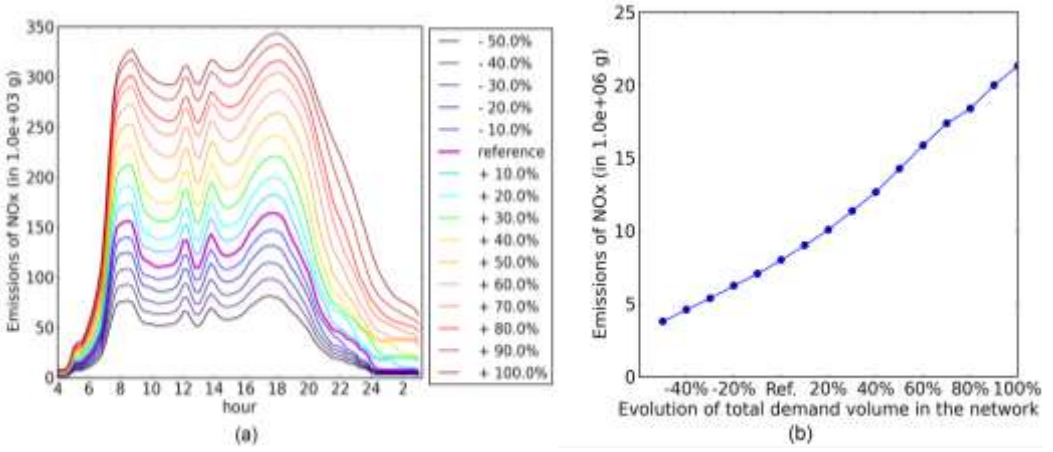

Figure 13. Sensitivity of the total emissions of the network to the total demand volume. (a) evolution for the whole day (in 10^3 g), (b) evolution of the total vehicle travel time in the whole network (in 10^6 g).

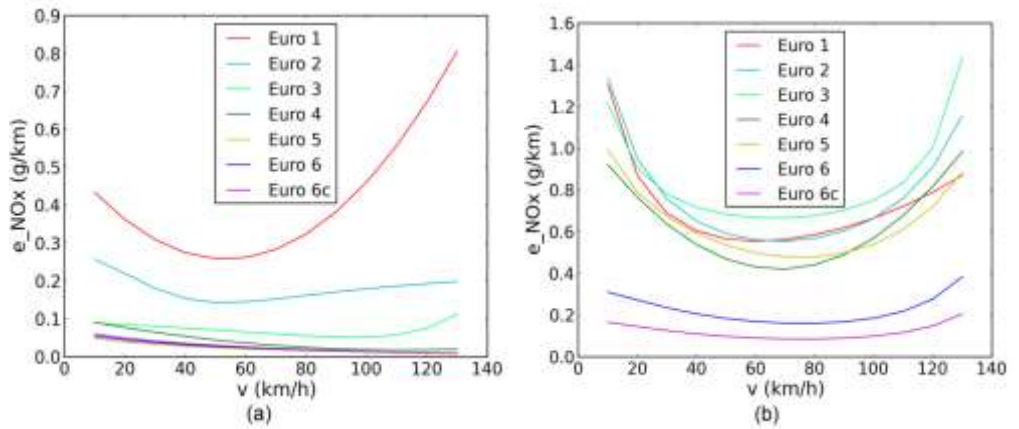

Figure 14: Sensitivity of hot emission factor of passenger cars for NOx to the average speed of (a) Gasoline passenger car, and (b) Diesel passenger car

5.2 Links' speed limit

This sub-section analyzes the sensitivity of traffic emission to the road's average speed in a more direct way. The maximum authorized speed of each road has been decreased by 5%, 10%, 15%, 20%, 25%, 30%, 35%, 40%, 45%, and 50%. It is

found that the total vehicle travel time and the network total emissions are less sensitive to the speed limitation than to the total demand, as shown in Figure 15 and Figure 16. Figure 16 (b) shows that the variation of the total emissions is not monotonic with the speed limitation. A minimum is reached for a decrease of 25%. For higher limitation of the speed, more emissions are released. We observe that limiting the link's speed does not strongly change the traffic flow in the network. The emissions follow the same non-monotonic trend as in Figure 14, and the variation of the amplitude depends on the vehicle fleet.

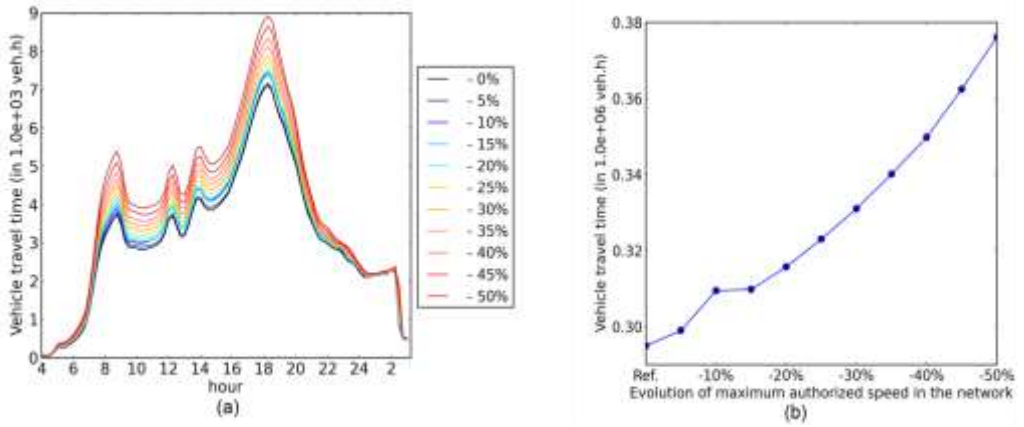

Figure 15: Sensitivity of total vehicle travel time to the links' speed limit. (a) temporal profile for the day (in 10^3 veh·h), (b) daily total value (in10^6 veh·h).

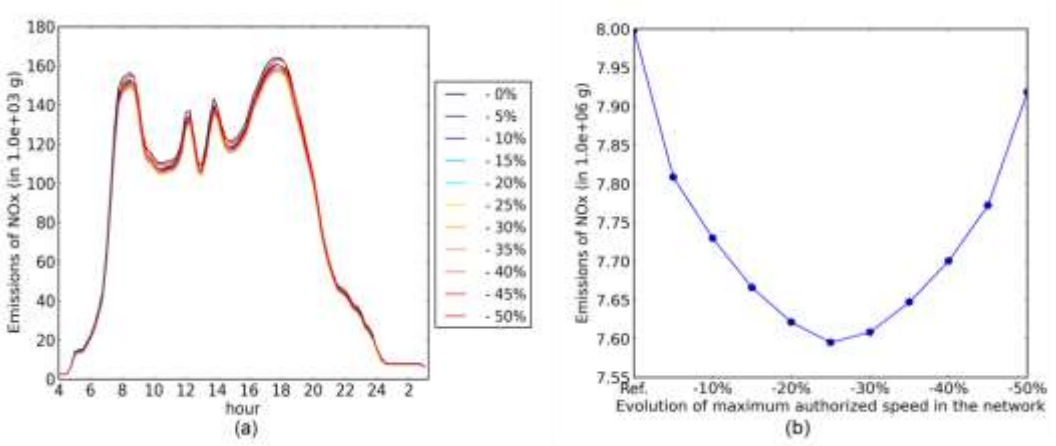

Figure 16: Sensitivity of the networks' total emissions to the links' speed limit. (a) temporal profile for the day(in 10^3 g), (b) daily total value(in 10^6 g).

5.3 Vehicle fleet composition

5.3.1 Effects of vehicle emission Euro standards

In this subsection, we divide passenger cars into two big categories: (i) the "Euro 4 +" vehicles with Euro standards of Euro 4 and higher, (ii) the "Euro 3 – "

vehicles with Euro standards from pre-Euro to Euro 3. In the reference simulation, the percentage of "Euro 4 +" vehicles is about 42.3% for passenger cars. For the sensitivity study, we increase the percentage of "Euro 4 +" cars from 42.3% to 80%. Within each category, we keep the same distribution of car standards. Figure 17 (a) shows that the NOx emissions decrease when the proportion of "Euro 4 +" category increases.

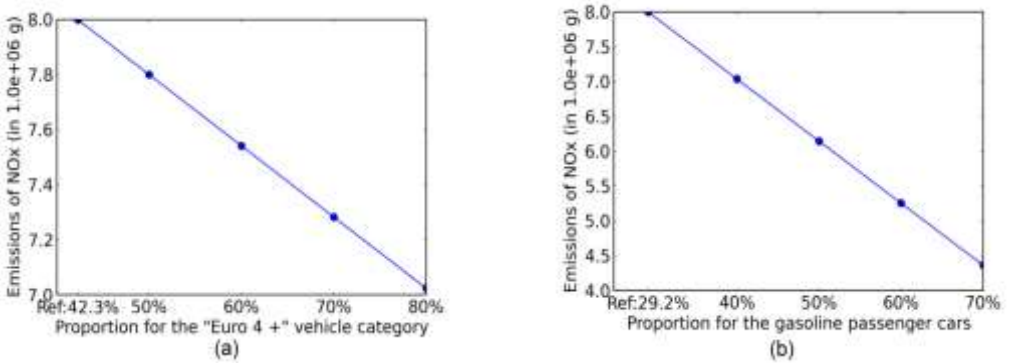

Figure 17: Sensitivity of total emissions of NOx to (a) Euro Standard and (b) vehicle fleet type.

5.3.2 Effects of the proportion for gasoline passenger cars and diesel passenger cars

In the reference case, the percentage of diesel passenger cars is 70.6% and that of gasoline passenger cars is 29.2%. We increase the proportion of gasoline passenger cars from 30% to 70% with steps by 10%. The results in Figure 17 (b) show that we can decrease the total NOx emission of 45% by doubling the percentage of gasoline passenger cars.

6 Conclusions

In this study, we have presented a simulation chain for emission calculations combined with a dynamic traffic assignment model called LADTA, and the COPERT IV method. The case study is carried out for a typical working day during non-vacation period for the agglomeration of Clermont-Ferrand. We have firstly analyzed users' travelling behavior in the network during the year and then used this information to calibrate and evaluate LADTA. The emission calculations are based on traffic flow results of LADTA for each link during every 15 minutes for the day. At last, we studied the sensitivity of the emissions to LADTA model and COPERT inputs.

Both the vehicle travel time and the total emissions increase with the total demand volume onto the network. The total vehicle time grows increasingly fast when total demand increases linearly, which leads to congestions. However, the non-linearity of emissions evolution is less significant since the decreased average speed may lead to the decrease of emission factors of NOx.

The variation of the link speed has less influence on the network total vehicle travel time and total emissions. As we decrease the links' speed limits, the total emissions firstly decrease and then increase. The minimum value is reached when the speed decreases by about 25%. This is mainly due to the influence of vehicle travel speed on the hot emission factors of NOx.
It is also found that the total emissions of NOx are sensitive to the vehicle fuel type as well as the Euro emission standards: emissions decrease strongly when we increase the percentage of gasoline passenger cars or vehicles with European emission standard of Euro 4 and higher.
This study shows the importance to take into account the congestion phenomenon by using a dynamic traffic assignment model. The emissions are very sensitive to the traffic flow, which can be increased immediately within a quarter of an hour. The static assignment model during peak hours or with separate hours may not be sufficient. Furthermore, the sensitivity analysis shows that when the total traffic demands change, emissions can change non-linearly. The actual variation of the total demand from one day to another might be significant enough to trigger large emission variations. In further studies, we will take into account the distribution of vehicle speed for emission calculations during heavy traffic periods, in order to better handle vehicles' unstable stopping and starting on congested links. Meanwhile, we will improve LADTA model to reduce its spatial errors. For example, we can apply different temporal profiles to different kind of O-D pairs for generating the input dynamic O-D matrix.

ACKNOWLEDGEMENTS. This work is funded by the French National Research Agency (Agence Nationale de la Recherche, i.e. ANR), project ESTIMAIR. The City of Clermont-Ferrand provided the traffic flow observational data. SMTC provided the modeled network, the static O-D matrix and a static traffic assignment for Clermont-Ferrand.

References

[1] Airparif, Inventaire regional des émissions en Île-de-France, Paris, (2014), p5.

[2] J. Wardrop, Some theoretical aspects of road traffic research, Proceedings of the Institution of Civil Engineers, **1(3)**, (1952), 325 – 362.

[3] F. Leurent, "On network assignment and supply demand equilibrium: an analysis framework and a simple dynamic model," in *European Transport Conference (CD Rom edition)*, (2003a).

[4] V. Aguiléra and F. Leurent, Large Problems of Dynamic Network Assignment and Traffic Equilibrium: Computation Principles and Application to Paris Road Network, *Transportation Research Record,* **vol. 2132**, (2009),

122 – 132.

[5] N. Wagner, Dynamic equilibrium on a transportation network: mathematical porperties and economic application, Ph.D Thesis, 2012.

[6] Bureau of Public Roads, *Traffic Assignment Manual*, U.S. Dept. of Commerce, Urban Planning Division, Washington D.C, 1964.

[7] J. Ortuzar and L. G. Willumsen, *Modeling Transportation*, 4th edition, Wiley, New York (2011), p353.

[8] M. Lighthill and J. Whitman, On kinematic waves, II: A theory of traffic flow on long crowded roads, *Proceeding of Royal Society,* **vol. A229(1778)**, (1955), 317 – 345,.

[9] P. Richards, Shock waves on the highway, *Operations Research,* **vol. 4**, (1956), 42 – 51.

[10] N. Geroliminis and C. Daganzo, Existence of urban-scale macroscopic fundamental diagrams: some experimental findings, *Transportation Research Part B,* **vol. 42(9)**, (2008a), 759 – 770.

[11] W. Vickrey, Congestion theory and transport investment, *American Economic Review,* **vol. 59**, (1969), 251 – 261.

[12] EMEP/EEA, *air pollutant emission inventory guidebook*, 1.A.3.b. Road transport, (2013), 40 – 66.

[13] M. André, A. Roche and K. F. Moore, Statistiques de parcs et trafic pour le calcul des émissions transports routiers en France, Report IFSTTAR-LTE, (2013), 88 – 89.